Electronic-charge displacement around a stacking boundary in SiC polytypes

A. Qteish,* Volker Heine, and R. J. Needs
Cavendish Laboratory, University of Cambridge, Madingley Road, Cambridge CB3 0HE, United Kingdom
(Received 16 October 1991)

We present self-consistent pseudopotential calculations of the charge-density redistribution around an effectively isolated stacking boundary (stacking fault) and a stacking boundary in 6*H* SiC. The major result is that the dipole setup is not centered on the central bond but nearly on the adjacent C atom, and the disturbance to the charge density ranges about 3.5 Å on either side. In light of these calculations, we interpret the magic-angle-spinning NMR data concerning the inequivalent Si and C sites, the spontaneous polarization, and the structural relaxation in SiC polytypes.

I. INTRODUCTION

The structures of SiC polytypes can be viewed as stackings of hexagonal SiC double layers on top of one another along what would be the [111] direction of the cubic zinc-blende (3*C*) form. Each double layer can be stacked in one of two ways. About 200 different SiC polytypes have been found, and the most common forms are 4*H*, 6*H*, and 15*R* (Ramsdell[1] notation will be used throughout this work). In all of these polytypes, except the 3*C* form, symmetry allows for the existence of inequivalent Si—C bonds which, in turn, allows for bond-to-bond charge transfer and hence structural relaxation.

The structural properties of SiC were the subject of several experimental investigations using magic-angle-spinning (MAS) NMR,[2,3] photoluminescence,[4–6] and electron-spin-resonance measurements.[7] The work of Choyke and co-workers[4–6] and Woodbury and Ludwig[7] on nitrogen impurities in SiC (which occupy C sites), has shown that there are three and four (or possibly five) inequivalent sites for C in 6*H* and 15*R* SiC, respectively. In spite of this information, it has been tacitly assumed that there are only two different Si or C sites in SiC.[8,9] Recent MAS-NMR measurements have supported the above findings that there are three different Si or C sites in 6*H* SiC; three and four different Si and C sites, respectively in 15*R* SiC.[2,3] The discrepancy between the number of inequivalent Si and C sites in 15*R* SiC is unexpected (from a geometrical point of view one expects them to be identical in any polytypic structure) and cannot be explained using the model proposed by Hartman *et al.*,[2] which assumes a fixed interaction range of 5 Å around a Si (or C) site. This model, on the contrary, gives identical numbers of distinct sites for the two atomic species. To the best of our knowledge, there is only one theoretical investigation[10] of the structural relaxation which covers 2*H*, 4*H*, 6*H*, and 15*R* SiC polytypes, which used a self-consistent pseudopotential method. These calculations have revealed interesting features about the relaxation of these polytypes, most notably the relaxation of the C atom near the stacking boundary (hereafter referred to as a boundary) which was difficult to explain, and the additivity of the forces in the 4*H*, 6*H*, and 15*R* forms. The above experimental and theoretical findings seem to suggest that a comprehensive and simple understanding of the structural properties of SiC polytypes can be achieved.

Another related property is the spontaneous polarization (hereafter referred to as the polarization) which results from both displacement of the electronic-charge density ρ and the ionic relaxation. The polarization in 2*H* SiC has been studied very recently by the present authors,[11] using a supercell approach proposed by Posternak *et al.*[12] It has been found that the polarization in 2*H* SiC is mostly due to the disturbance to ρ. However, there are still important questions to be answered, such as, what is the nature of the dipole setup by an isolated boundary, and can the polarization in a SiC polytype be understood as a superposition of dipoles due to each of its boundaries?

The aim of this work is to calculate the disturbance to ρ around an isolated boundary in SiC, and to investigate its range and the resulting electric dipole. Having obtained this information, we shall try to interpret the above MAS-NMR data, the internal structural relaxation, and the polarization in SiC polytypes. To this end, we have performed self-consistent pseudopotential calculations for unrelaxed 6*H* and 8*H* SiC. In the latter structure the boundaries are found to be effectively isolated. The main result is that the disturbance to ρ around a boundary is not centered on the central bond but very close to the adjacent C atom, and ranges about 3.5 Å on either side. This range contains two Si and three C atomic layers. We conclude that the number of different Si and C sites in all SiC polytypes taken together is four and eight, respectively. This conclusion is consistent with and explains the number of different sites obtained from MAS-NMR spectra for 15*R* SiC.[2,3] Furthermore, we have found that the disturbance to ρ, calculated as the difference between the planar average charge density normal to the stacking direction of the 6*H* and 3*C* forms, explains the structural relaxation in SiC polytypes. The electric dipole is found to be quite localized around the boundary, which permits the calculation of the polarization in most SiC polytypes without the need for a reference material.[12] The calculated polarization in 6*H* and 8*H* SiC is 9.49×10^{-3} and 6.91×10^{-3}, respectively. Therefore, we conclude that the polarization in SiC poly-

types can be interpreted as a superposition of localized dipoles due to the stacking faults, and hence varies almost linearly with the degree of hexagonality. In the $2H$ and $9R$ SiC the dipole-dipole interactions are found to be rather weak.

The rest of the paper is organized as follows. In Sec. II we give details of the calculations and the results for ρ and its disturbance due to the boundaries in $6H$ and $8H$ SiC. Section III is devoted to the discussion of the number of different Si or C sites and the MAS-NMR spectra. In Sec. IV we discuss the nature of the electric dipole due to an isolated boundary and the linearity of the polarization in SiC polytypes with the degree of hexagonality. In Sec. V we relate the calculated disturbance of the charge density to the ionic relaxation in SiC polytypes, and explain the large relaxation of the C ions near the boundaries. Finally, in Sec. VI we summarize our main results and conclusions.

II. VALENCE CHARGE-DENSITY REDISTRIBUTION

To study the disturbance to the charge density ρ due to an isolated stacking boundary in SiC polytypes, we have performed self-consistent pseudopotential calculations for the unrelaxed $6H$ and $8H$ forms (i.e., with all atoms in their ideal tetrahedral positions and lattice spacing equal to that of the cubic form). Other computational details are exactly as given in Ref. 11.

In Fig. 1 we show a contour plot of ρ along the bond chain of $6H$ SiC. From this figure one can hardly see any difference in the bond charge-density distribution at the boundaries. This is exactly what we expect, since the disturbance to ρ is too small.[11] To highlight the disturbance to ρ, we show in Figs. 2 and 3 the macroscopic average charge density $\bar{\rho}$ of $6H$ and $8H$ SiC, respectively, calculated using the running macroscopic averaging technique of Baldereschi, Baroni, and Resta.[13] In Figs. 2 and 3 we also show the averaged total potential, $\bar{V}_{\rm tot}$, for the two structures respectively. The $\bar{V}_{\rm tot}$ is defined as the sum of the averaged Hartree, exchange correlation, and the local parts of the ionic potentials. The important features to note are (i) the disturbance to ρ, manifested by the deviation of $\bar{\rho}$ from its value in $3C$ SiC (8.0 e/unit cell of two atoms), $\Delta\bar{\rho}$, is not centered on the central bond but nearly on the adjacent C atom and ranges about 3.5 Å on either side; (ii) the similarity of the $\bar{\rho}$ profile around the boundaries in the two structures; (iii) although the disturbance to ρ is rather extended, the resulting dipole seems to be localized (in the regions where the slope of $\bar{V}_{\rm tot}$ is positive; see Sec. IV) and lies across the transverse bond, as predicted in Ref. 11. We will show in the next three sections that these features have important consequences for

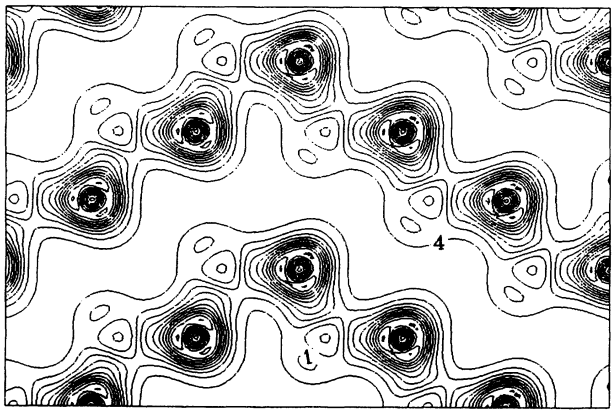

FIG. 1. Contour plot of the valence charge density of unrelaxed $6H$ SiC (see Fig. 2), in the plane of the bond chains, normalized to eight electrons per unit cell (i.e., multiplied by a factor of $\frac{1}{6}$). The successive contours are equally spaced and are separated by 3 electrons/unit cell.

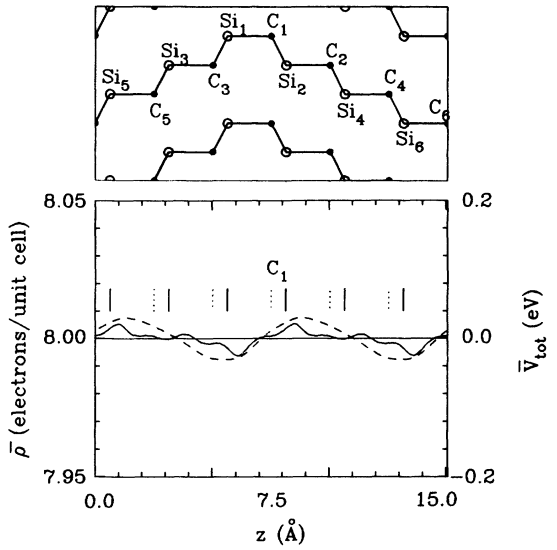

FIG. 2. Upper panel: Si—C bond chains along the stacking direction in unrelaxed $6H$ SiC. The Si and C atoms are numbered. Lower panel: Averaged charge density (solid lines) $\bar{\rho}$ and averaged total potential (dashed lines) $\bar{V}_{\rm tot}$ of $6H$ SiC. The projection of Si and C atomic layers are shown by short vertical solid and dotted lines, respectively.

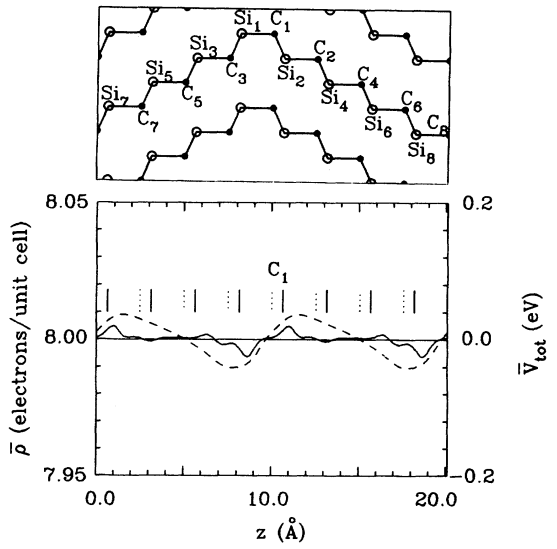

FIG. 3. Same as in Fig. 2 but for $8H$ SiC.

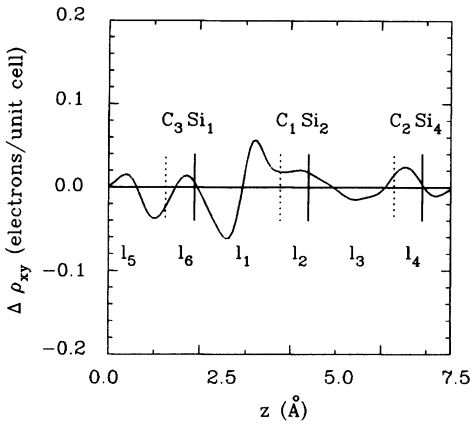

FIG. 4. Difference of the charge density averaged in planes normal to the stacking axis (the x-y plane) $\Delta\rho_{xy}(z)$ between unrelaxed $6H$ and $3C$ SiC. The positions of the Si and C atomic layers are shown by vertical solid and dotted lines, respectively. The bonds are labeled as in Ref. 10.

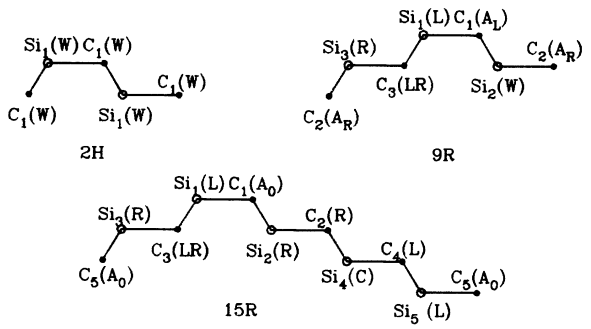

FIG. 5. Si—C bond chains along the stacking direction in $2H$, $9R$, and $15R$ SiC.

the structural properties and on the polarization of SiC polytypes.

We show in Fig. 4 the difference between the charge densities of the $6H$ and $3C$ forms averaged in the planes normal to the stacking direction, $\Delta\rho_{xy}$, around a stacking fault. This is effectively a deconvolution of $\Delta\bar{\rho}$ around the boundaries in $6H$ SiC shown in Fig. 2. It is worth mentioning that this deconvolution was performed exactly from the charge densities of the two structures. The advantage is that $\Delta\rho_{xy}$ provides a better resolution for the disturbance to ρ which is necessary to interpret the ionic relaxation in SiC polytypes (see Sec. V). By comparing Figs. 2 and 4, one can see that the fact that the disturbance to ρ is centered near the C atom is still valid, even though the maximum of $\Delta\rho_{xy}$ lies on the central bonds.

III. INTERPRETATION OF THE MAS-NMR SPECTRA

MAS-NMR spectroscopy has proved to be a fruitful probe in studies of local-site environments. This is because the chemical shifts are very sensitive to any chemical (number and type of atoms) or structural changes (ionic relaxation) around the nuclei under consideration. Recently, this technique has been applied successfully to study the structural properties of SiC polytypes,[2,3] namely, the number of different Si or C sites in $3C$, $6H$, and $15R$ SiC. In this section we summarize and interpret the data obtained for these polytypes and predict the number and intensity of the peaks in the spectra of other SiC polytypes.

Geometrically there are, respectively, one, three, and five different Si (or C) sites in $3C$, $6H$ (see Fig. 2), and $15R$ SiC (see Fig. 5). For $3C$ and $6H$ SiC, the MAS-NMR measurements have revealed exactly that for $3C$ SiC only the ^{29}Si spectrum has been obtained and a single peak is found at -18.3 (Ref. 2) or -16.1 (Ref. 3) ppm. For $6H$ SiC, three peaks of equal intensity have been found in the ^{29}Si and the ^{13}C spectra. The three ^{29}Si peaks lie at -13.9, -20.2, and -23.2 ppm,[2] or -14.3, -20.4, and -24.9 ppm,[3] whereas the three ^{13}C peaks lie at 15.2, -20.5, and -24.1 ppm.[2] The interpretation of the $15R$ SiC spectra is not as straightforward since only three peaks[2,3] in the ^{29}Si spectrum and four peaks[2] in the ^{13}C spectrum have been found. Moreover, the relative intensities of these peaks are also different; they are in the ratios 1:2:2 and close to 2:1:1:1, respectively. The locations of the peaks are found to be very close to those for $6H$ SiC, at -14.9, -20.8, and -24.4 ppm,[2] or -14.6, -20.5, and -24.1 ppm (Ref. 3) for ^{29}Si, and at 13.3, 16.0, 20.7, and 22.7 ppm for ^{13}C.[2] Note that the ^{13}C peak at 13.3 ppm does not exist in $6H$ SiC. One should also mention that in the ^{29}Si spectrum of $15R$ SiC of Guth and Petuskey,[3] the middle peak at -20.5 ppm splits into two very close peaks, which suggests that it corresponds to two very similar Si sites, a feature which was not observed by Hartman *et al.*[2]

There are several intriguing conclusions to be drawn from the above experimental data. (i) The peaks in the ^{29}Si spectrum and three of the peaks in the ^{13}C spectrum of $15R$ SiC lie almost in the same positions as the corresponding peaks in the spectra of $6H$, SiC. This suggests that they correspond to very similar local Si and C environments in the two polytypes. (ii) The number of peaks in the spectra of $15R$ SiC is smaller than 5 (the number of geometrically different sites). This can only happen if the effects of the boundaries are short ranged and allow sites Si_1 and Si_5, and Si_2 and Si_3 (see Fig. 5) to be identical, giving an intensity ratio of 1:2:2. (iii) The fourth peak at 13.3 ppm in the ^{13}C spectrum of $15R$ SiC is a mystery and, as argued by Hartman *et al.*,[2] it could be either a genuine ^{13}C peak or it could due to an unknown impurity. However, we believe that, because of the high sensitivity of the MAS-NMR spectra, the latter explanation is highly unlikely—it is difficult to see how another kind of atom with a very different charge-density distribution and ionic relaxations around it can have a resonance frequency very close to that of C atoms. (iv) The splitting of the middle peak in the ^{29}Si spectrum of Guth and Petuskey[3] suggests that one pair of the doubly degenerate sites (Si_1 and Si_5, or Si_2 and Si_3) feels the effects of the second-nearest boundary. Although Guth and Petuskey have concluded that it is the latter pair, on the grounds that they are closer to the second-nearest boundaries, we be-

lieve that such a conclusion is premature and cannot be decided using geometrical arguments only. This is because of the fact that the location of the effective boundary is not well defined.[11] (v) From (i) and (ii) one can conclude that the number of different Si or C sites in SiC polytypes is very limited (assumed to be four in Refs. 2 and 3; see below), in spite of the large number of distinct polytypes.

To explain the above experimental data, Hartman *et al.*[2] have introduced a model which assumes an effective interaction range of 5 Å around a central Si (or C) atomic layer. This range contains one atomic layer of the same kind and two of the other on either side of the central layer. They have shown that there are only four inequivalent stacking configurations of the atomic layers within such a range and, therefore, they argued that there are only four different Si or C sites in SiC polytypes. Guth and Petuskey[3] have independently arrived at a similar explanation. There are two major weaknesses in this model. (i) Fixing the interaction range to 5 Å while the next atomic layer is at 5.02 Å is quite unrealistic; (ii) although the model explains rather well the number of different Si sites in the SiC polytypes studied, this model cannot account for the observed number of different C sites in 15*R* SiC.

To interpret the MAS-NMR spectra, we have adopted a somewhat different approach to the above geometrical one. The distinct Si or C sites result from the presence of the boundaries in SiC polytypes which causes electronic charge-density redistribution and ionic relaxation. The former is the driving force for the latter and, therefore, we content ourselves with studying only the range of the disturbance to ρ due to an isolated boundary in SiC polytypes. From Figs. 2 and 3 it is evident that the boundaries in 8*H* SiC are effectively isolated and the effective range of each of them contains five atomic layers, namely the central C layer and two atomic layers on either side (C_1, Si_1, C_2, Si_2, and C_3 in Figs. 2 and 3). The next Si layers are very slightly affected by the boundary: $\Delta\bar{\rho}$ at these sites are only about 10% of its maximum or minimum values near the boundaries. Whether to neglect such small effects and consider them as 3C SiC sites or to treat them as different sites is a rather delicate matter. However, we have found that treating them as 3*C* SiC sites explains the MAS-NMR data very well. Therefore, we shall consider the above five sites as the only sites affected by the boundary. Because of the asymmetry of Si (and C) sites, the affected sites are different from one another and, in turn, are different from the corresponding sites in 3*C* SiC.

From the discussion given in the previous paragraph, we can conclude that there is a total of only four different Si sites and up to eight different C sites in SiC polytypes, not all usually occurring in any one polytype. The four different Si sites are as follows: (1) sites affected by a boundary from the left (like site Si_2 in Figs. 2 and 3), (2) sites affected by a boundary from the right (like site Si_3 in Figs. 2 and 3), (3) the Si sites in 3*C* SiC (unaffected by any boundary), and (4) the Si sites in 2*H* SiC (affected by two boundaries; see Fig. 5). As for the eight different C sites, four of them (1–4) can be defined as those for Si, and the other four are (5) sites like C_3 of 15*R* in Fig. 5 affected by two boundaries centered at the first nearest C neighbors along the stacking direction; (6) central C sites not affected by any other boundary (like site C_1 in Figs. 2 and 3); (7) central C sites affected by another boundary from the left (like site C_2 of 9*R* SiC in Fig. 5); and (8) central C sites affected by another boundary from the right (like site C_1 of 9*R* SiC in Fig. 5). The four different Si sites will be referred to as types *L*, *R*, *C*, and *W*, respectively, and those for C as types *L*, *R*, *C*, *W*, *LR*, A_0, A_L, and A_R, respectively. To check the soundness of this classification we count the number of different Si and C sites in 15*R* SiC (see Fig. 5 and Table I). We found that in this polytype there are three distinct Si sites of types *C*, *R*, and *L* with frequency 2:4:4, respectively, and four distinct C sites of types A_0, *L*, *R*, and *LR* with frequency 4:2:2:2, respectively, which explains very nicely the MAS-NMR spectra[2,3] of 15*R* SiC. In Table I we give the number and types of the different Si and C sites in some SiC polytypes. The larger number of different C sites than that of

TABLE I. Number of sites of each Si (and C) type (see text) in some SiC polytypes. The average resonance shift (in ppm) of some different site types are also shown (see text).

		Si sites				C sites							
Ramsdell	Zhdanov	*C*	*W*	*L*	*R*	*C*	*W*	*L*	*R*	*LR*	A_0	A_L	A_R
(Ref. 1)	(Ref. 15)	−15.6		−24.0	−20.3					13.3	22.7		
3*C*	∞	3				3							
2*H*	11		2				2						
4*H*	22			2	2					2	2		
6*H*	33	2		2	2			2	2		2		
8*H*	44	4		2	2	2		2	2		2		
9*R*	$(21)_3$		3	3	3					3		3	3
10*H*	3322	2		4	4			2	2	2	4		
14*H*	$(22)_2 33$	2		6	6			2	2	4	6		
15*R*	$(23)_3$	3		6	6			3	3	3	6		
19*R*	$(23)_3 22$	3		8	8			3	3	5	8		
20*H*	$(22)_3 44$	4		8	8	2		2	2	6	8		
21*H*	333534	9		6	6	3		6	6		6		
24*R*H	$(35)_3$	12		6	6	6		6	6		6		

Si can be understood as a consequence of the location of the effective boundary, a feature which was impossible to predict without the present detailed self-consistent calculations.

Finally, from Figs. 3 and 4 we notice that site Si_4 appears to be slightly more affected by the boundary than Si_3. We believe that this could be the reason behind the splitting of the middle peak in the ^{29}Si spectrum of Guth and Petuskey.[3] Since the splitting is so small, it can be neglected as it was in Ref. 3 and the two sites can be considered as equivalent. However, the splitting helps in associating this peak with type R (site Si_1 of 15R SiC in Fig. 5 is slightly affected by the boundary centered at site C_5, whereas Si_5 is effectively unaffected by the more distant boundary at C_1). Similarly site Si_4 (of type C) of this figure will also be slightly affected by the boundary centered at site C_1, but this will not result in a splitting since no other similar sites exist in the 15R SiC. From the relative intensity we can then associate the peaks at -14.9 and -24.4 ppm with types C and L, respectively. As for the peaks in the ^{13}C spectrum of 15R SiC, the two peaks at 13.3 and 22.7 ppm can be easily associated, from the relative intensity and the absence of the former from the spectrum of 6H SiC, with types LR and A_0, respectively. More MAS-NMR measurements for other SiC polytypes are needed to obtain full information about the chemical shifts of the other types of different sites, in particular, for the 2H, 4H, and 9R polytypes.

IV. SPONTANEOUS POLARIZATION

In this section we shall focus on the nature of the electric dipole due to an isolated stacking boundary, the polarization in 6H and 8H SiC, and the linearity of the polarization with respect to the degree of hexagonality. As pointed out in Sec. I, the polarization results from both the disturbance to ρ and the ionic relaxation. In Ref. 11 we have shown that the polarization in 2H SiC is mainly due to the disturbance to ρ. Since the ionic relaxations are not included in the present study, only the electronic contribution to the polarization will be discussed.

The polarization in pyroelectric materials is very difficult to determine both experimentally and theoretically. It leads to an electric potential difference between the two ends of a finite crystal, along the polarization axis. This is usually compensated for by attracting charges from the air, and/or by the migration of electrons and holes due to impurities from inside the material. Furthermore, the polarization in a finite slab depends on the state of the crystal surfaces, which makes the polarization dependent on a sample preparation and external conditions. On the other hand, the use of Born–von Karman boundary conditions to recover the thermodynamic limit makes the polarization inaccessible to first-principles calculations performed for a unit cell of a bulk material.

Very recently an approach has been proposed by Posternak *et al.*[12] They have shown that the polarization in a slab of pyroelectric material, with faces normal to the polarization axis, can be determined as the difference between the polarization in such a slab and in a similar slab of a reference material, chosen to be the 3C form which has zero bulk polarization, by symmetry. The two structures are perfectly matched at the (111) interface, which is a very natural boundary, indeed, the only sensible one, for defining the polarization. The two slabs are then infinitely repeated to allow for a quantum-mechanical treatment of the problem in a supercell geometry. Because of the above particular choice of the reference material, the calculated polarization does not depend on the truncation of the polarized slab and other surface-induced effects. We will show below that in some particular cases the polarization can be extracted directly from bulk self-consistent calculation, i.e., without the need for a reference material.

The extent and the direction of the electric dipole due to an isolated boundary can be obtained from the information provided by Figs. 2 and 3. As is evident from these two figures, $\bar{V}_{\rm tot}$ has a sawtooth shape in both 6H and 8H SiC, similar to that obtained for the artificial supercell used to calculate the polarization in 2H SiC.[11] The sawtooth shape is a result of the electric dipoles due to the boundaries and the depolarization field due to the use of periodic-boundary conditions. Therefore, the regions where $\bar{V}_{\rm tot}$ has a positive slope are the ones with nonzero polarization, and the intermediate cubic regions (where $\bar{V}_{\rm tot}$ has a negative slope) act here as the reference material needed in the Posternak *et al.*[12] approach. The use of $\bar{V}_{\rm tot}$ instead of $\bar{V}_H$ has been justified in Ref. 11. From the width of the polarized regions we conclude that the electric dipole due to an isolated boundary is quite localized. Moreover, it lies across the transverse C_1—Si_2 bond, approximately centered at C_1 and pointing toward the left, see Figs. 2 and 3. The location and direction of this electric dipole are consistent with the predictions made in Ref. 11, and hence supports our choice of the interface between the 3C and 2H regions in the supercell used in Ref. 11.

The localization of the electric dipoles due to the boundaries allows for direct determination of the polarization in SiC polytypes, such as 6H and 8H, without the need for a reference material.[11,12] To determine the polarization in such polytypes, it is most convenient to average it over the unit cell. By doing so, the macroscopic electric field due to the average polarization becomes equal in magnitude and opposite in sign to the depolarization field. Therefore, the intrinsic polarization[11] $P_{\rm int}$ of such polytypes is given by

$$P_{\rm int} = -\epsilon_0 \epsilon_\infty E_{\rm dep} = -\epsilon_0 \epsilon_\infty \frac{\partial \bar{V}_{\rm tot}(C)}{\partial z} , \tag{1}$$

where $E_{\rm dep}$ is the depolarization field $\bar{V}_{\rm tot}(C)$ is the averaged total potential well inside the intermediate cubic regions. The calculated polarization in 6H and 8H SiC is 9.49×10^{-3} and 6.91×10^{-3} C/m^2, respectively. It is important to note that the ratio between the polarization in 8H and 6H SiC is 0.73, while the ratio between the relative number of boundaries in the two polytypes is 0.75. This indicates that the polarization in SiC polytypes varies linearly with the degree of hexagonality, at least in the limit of a small degree of hexagonality, and hence the polarization in these polytypes can be interpreted as a su-

perposition of electric dipoles due to their stacking faults. This result is of great importance since it justifies the use of the localized dipoles in the classical treatment of the polarization, at least in SiC polytypes.

To see how much the dipole-dipole interactions affect the polarization in $2H$ SiC, we extrapolate the above results to calculate the polarization in this polytype, giving 2.80×10^{-2} C/m^2 compared to 3.33×10^{-2} C/m^2 obtained in Ref. 11. Therefore, we conclude that the dipole-dipole interactions in $2H$ SiC have a rather weak effect on the polarization in this polytype, and hence the polarization in all SiC polytypes, to a very good approximation, varies linearly with the degree of hexagonality. It is worth mentioning again that only the electronic contribution to the polarization is discussed here.

V. STRUCTURAL RELAXATION

The ionic relaxations of $2H$, $4H$, $6H$, and $15R$ SiC have been studied using a self-consistent pseudopotential technique, by minimizing the total energy of those polytypes with the help of the calculated forces on the ions and the stress tensor.[10] The calculated bond lengths and bond angles were, generally speaking, in good agreement with the experimental results. Although the aim of that work was to investigate the role of the ionic relaxations on the stabilization of these polytypes, it also revealed other interesting features about the ionic relaxations in SiC polytypes, most notably, the large relaxation of the C ions (C_1 in Figs. 2–5) adjacent to the boundaries. Before relaxation, the calculated forces on these ions were found to be very large compared to those on the other ions. Despite the attempt made in Ref. 10 to explain such large forces, they remained not fully understood. In the following we check whether the calculated changes in the bond-charge densities agree with the calculated and measured ionic relaxations, and identify the reason for the large forces.

In Table II, we give the excess bond-charge densities, calculated by integrating over each bond the difference in the planar average charge density of $6H$ and $3C$ SiC shown in Fig. 4. For comparison we show the same table the calculated[10] and measured[14] percentage differences of bond lengths of $6H$ SiC from the ideal tetrahedral value. Table II shows, as expected, that there is a transfer of charge from the weaker (longer) longitudinal bonds to the stronger (shorter) transverse bonds. Furthermore, the similarity of the profile of $\Delta\bar{\rho}$ around the boundaries in SiC polytypes is consistent with the fact that the transverse bonds are always shorter than or equal to (far from the boundaries) the longitudinal ones. This provides further evidence for the consistency of our results with other theoretical and experimental data.

TABLE II. Excess bond charge density $\Delta\rho$ and percentage difference in the bond length Δb of $6H$ SiC (see Fig. 4) bonds with respect to that of $3C$ SiC.

Bond	$\Delta\rho$ (e)	Δb (Theor.) (Ref. 10)	Δb (Expt.) (Ref. 14)
l_1	−0.0027	0.404	0.33
l_2	0.0052	−0.023	−0.09
l_3	−0.0018	0.104	0.33
l_4	0.0041	−0.066	−0.14
l_5	−0.0061	0.102	0.17
l_6	0.0005	−0.086	−0.09

The reason for the large forces, found in Ref. 10, on the C_1 atoms in Figs. 2–5 now seems to have an obvious explanation. From those figures one can see that the C_1 atom lies in the middle of the effective range of the boundary where the macroscopic electric field, E, is a maximum. The forces on the ions F_i are related to E by

$$F_i = q_i^* E_i \ , \tag{2}$$

where q_i^* and E_i are the effective charge of and the electric field around ion i. Since $|q_i^*|$ is expected to be the same for all the C and Si ions, we conclude therefore that the large forces on the above C ions are due to their central position in the effective ranges of the boundaries.

VI. CONCLUSIONS

We have performed self-consistent pseudopotential calculations to study the disturbance to the electronic-charge density ρ around an isolated stacking boundary in SiC polytypes. Two SiC polytypes, namely $6H$ and $8H$, have been used in this study. In $8H$ SiC the boundaries are found to be effectively isolated. Furthermore, we have used the calculated disturbance to ρ to (i) interpret the MAS-NMR data concerning the number of inequivalent sites for Si and C, (ii) readdress the questions of the nature of the electric dipole due to an isolated boundary, and the linearity of the spontaneous polarization with respect to the degree of hexagonality; (iii) explain some features of the ionic relaxation in SiC polytypes. In the following we summarize our main results and conclusions.

(1) The disturbance to ρ around an isolated boundary is found to be very weak and not centered on the boundary, as expected, but on the adjacent C atom. The latter is consistent with and explains the large forces on the central C atom calculated in Ref. 10. The effective range of a boundary is found to include two atomic layers on either side of its central C layer.

(2) The number of different Si and C sites in SiC polytypes is found to be four and eight, respectively. The types of the distinct sites have been defined, and the number and type of the different Si and C sites are tabulated, for several polytypes. Our results explain the number and relative intensities of the peaks in the MAS-NMR spectra of the chemical shifts of ^{29}Si and ^{13}C of $6H$ and $15R$ SiC.

(3) The electric dipole due to an isolated boundary is found to be quite localized, lying across the transverse bond (see Figs. 2 and 3) and pointing towards the C side.

(4) The localization of the electric dipoles due to the boundaries allows one to calculate the polarization in SiC polytypes, such as $6H$ and $8H$, without the need for a reference material used in the approach of Posternak *et al.*[12] This conclusion can be generalized to any pyroelectric material in which the polarized regions are well

separated from each other. The calculated intrinsic polarization in $6H$ and $8H$ SiC is found to be 9.49×10^{-3} and 6.91×10^{-3} C/m^2, respectively, and varies linearly with the degree of hexagonality. The effects of the dipole-dipole interactions are found to be rather weak even in polytypes with a high degree of hexagonality such as the $2H$ form.

(5) The bond-to-bond charge transfer (from longitudinal to transverse) is consistent with and explains the ionic relaxation in SiC polytypes.

ACKNOWLEDGMENTS

The authors are grateful to the Science and Engineering Research Council (U.K.) for financial support.

*Present address: Centre for Theoretical and Applied Physics, Yarmouk University, Irbid, Jordan.

[1]L. S. Ramsdell, Am. Mineral. **32**, 64 (1947).
[2]J. S. Hartman, M. F. Richardson, B. L. Sherriff, and B. G. Winsborrow, J. Am. Chem. Soc. **109**, 6059 (1987).
[3]W. J. Guth and W. T. Petuskey, J. Phys. Chem. **91**, 5361 (1987).
[4]W. J. Choyke and L. Patrick, Phys. Rev. **127**, 1868 (1962).
[5]W. J. Choyke, D. R. Hamilton, and L. Patrick, Bull. Am. Phys. Soc. **7**, 185 (1962).
[6]L. Patrick, Phys. Rev. **127**, 1878 (1962).
[7]H. H. Woodbury and G. W. Ludwig, Phys. Rev. **124**, 1083 (1961).
[8]A. R. Verma and P. Krishna, *Polymorphism and Polytypism in Crystals* (Wiley, New York, 1966).
[9]W. J. Weltnep, J. Chem. Phys. **51**, 2469 (1969).
[10]C. Cheng, V. Heine, and R. J. Needs, J. Phys. Condens. Matter **2**, 5115 (1990).
[11]A. Qteish, V. Heine, and R. J. Needs, Phys. Rev. B (to be published).
[12]M. Posternak, A. Baldereschi, A. Catellani, and R. Resta, Phys. Rev. Lett. **64**, 1777 (1990); M. Posternak, R. Resta, and A. Baldereschi (unpublished).
[13]A. Baldereschi, S. Baroni, and R. Resta, Phys. Rev. Lett. **61**, 734 (1988).
[14]A. H. Gomes de Mesquita, Acta Crystallogr. **23**, 610 (1967).
[15]G. S. Zhdanov, Comp. Rend. Acad. Sci. USSR **48**, 43 (1945).